Partial Disassembly of Peroxisomes

STEFAN E. H. ALEXSON, YUKIO FUJIKI, HELEN SHIO, and PAUL B. LAZAROW
The Rockefeller University, New York 10021. Mr. Alexson's permanent address is The Wenner Gren Institute, University of Stockholm, Stockholm, Sweden.

ABSTRACT Rat liver peroxisomes were subjected to a variety of procedures intended to partially disassemble or damage them; the effects were analyzed by recentrifugation into sucrose gradients, enzyme analyses, electron microscopy, and SDS PAGE. Freezing and thawing or mild sonication released some matrix proteins and produced apparently intact peroxisomal "ghosts" with crystalloid cores and some fuzzy fibrillar content. Vigorous sonication broke open the peroxisomes but the membranes remained associated with cores and fibrillar and amorphous matrix material. The density of both ghosts and more severely damaged peroxisomes was ~1.23. Pyrophosphate (pH 9) treatment solubilized the fibrillar content, yielding ghosts that were empty except for cores.

Some matrix proteins such as catalase and thiolase readily leak from peroxisomes. Other proteins were identified that remain in mechanically damaged peroxisomes but are neither core nor membrane proteins because they can be released by pyrophosphate treatment. These constitute a class of poorly soluble matrix proteins that appear to correspond to the fibrillar material observed morphologically.

All of the peroxisomal β-oxidation enzymes are located in the matrix, but they vary greatly in how easily they leak out. Palmitoyl coenzyme A synthetase is in the membrane, based on its co-distribution with the 22-kilodalton integral membrane polypeptide.

Peroxisomes of rat liver have long appeared to be membrane-bounded bags filled with homogeneous soluble contents, save for a paracrystalline, urate oxidase–containing core. Evidence in support of this view includes: (*a*) parallel release upon freezing and thawing of catalase, L-α-hydroxyacid oxidase, and D-amino acid oxidase (1); (*b*) similar distributions of these enzymes in differential, equilibrium density, and zonal centrifugations (2–4), including the presence of ~30% of each in soluble form in homogenates—this soluble activity was thought to be due to the breakage of ~30% of the peroxisomes during homogenization; (*c*) parallel behavior of newly synthesized and older peroxisomal proteins in fractionation and turnover experiments, suggestive of a single pool of proteins (4, 5).

In experiments with an antiserum raised against total rat liver peroxisomes, we found that several peroxisomal polypeptides are not present in soluble form in homogenates (Wong, L., and P. B. Lazarow, manuscript submitted for publication). These proteins appear to be neither integral membrane proteins (6) nor part of the core (7). What keeps them inside damaged peroxisomes? Where within the peroxisome are they located? One of these nonsoluble polypeptides is identified (8, 9) as the bifunctional protein catalyzing two reactions of the peroxisomal β-oxidation pathway (10). Several laboratories have studied the intraperoxisomal location of the β-oxidation enzymes and other enzymes, but with conflicting results (11–16).

We have investigated these questions by submitting purified peroxisomes to a variety of procedures intended to partially disassemble them. The effects were analyzed by analytical centrifugation, by electron microscopy, and by SDS PAGE. The enzymes selected for investigation include catalase, the most abundant protein in normal rat liver peroxisomes (1, 6) and urate oxidase, the major (if not only) constituent of the crystalloid core (1, 7, 17–19). We also studied palmitoyl-coenzyme A (CoA)[1] synthetase and enzymes of the β-oxidation system: acyl-CoA oxidase, β-hydroxyacyl-CoA dehydrogenase (which together with enoyl-CoA hydratase forms the bifunctional protein) and thiolase. The proteins selected for study include a set of polypeptides labeled *a–h* that have been the focus of other work (20) (Wong, L., and P. B. Lazarow, submitted for publication) and two integral membrane polypeptides (IMPs) with masses of 22 and 15 kilodaltons (kD) (6). The results of these investigations, some of which have been communicated in abstract form (21), have considerably changed our view of peroxisome structure.

[1] *Abbreviations used in this paper:* CoA, coenzyme A; IMP, integral membrane polypeptide.

THE JOURNAL OF CELL BIOLOGY · VOLUME 101 JULY 1985 294-305

MATERIALS AND METHODS

Purification of Peroxisomes in a Vertical Rotor

A light mitochondrial (lambda) fraction was prepared from the livers of four normal, female Sprague-Dawley rats (injected with Triton WR-1339) according to Leighton et al. (3). About 1.2 ml of lambda fraction (~100 mg protein/ml) was layered on each of two 14.5-ml linear sucrose gradients (density span from 1.15 to 1.27 g/ml) in Sorvall TV-865B rotor tubes (DuPont-Sorvall, Newtown, CT). Each gradient rested on a 1-ml cushion of 1.32 g/ml sucrose and the samples were overlaid with 1 ml of 0.25 M sucrose. All sucrose solutions contained 3 mM imidazole/HCl, pH 7.2, 0.1% ethanol, and 1 mM EDTA. Centrifugation was carried out at 50,000 rpm (200,000 g_{av}) for ~40 min at 10°C in a Sorvall OTD-75 centrifuge (DuPont-Sorvall) equipped with an automatic rate controller for slow acceleration and deceleration below 1,000 rpm. Total centrifugation was controlled by an $\omega^2 t$ integrator accessory to give $\int \omega^2 dt = 6.66 \times 10^{10}$ s^{-1}. This value was chosen to obtain the same effective centrifugation used by Leighton et al. (3), after correcting for the difference in rotor geometry, which is sufficient for the peroxisomes to reach their equilibrium density.

Experimental Procedures

Fresh peroxisomes (7–12 mg/ml in dense sucrose solution from the preparative isopycnic gradient) were diluted fivefold, treated in various ways described below, and layered on top of a second sucrose gradient (density span, 1.06–1.27 g/ml). The gradient solutions contained 3 mM imidazole, pH 7.2, 0.1% ethanol, and 1 mM dithiothreitol (required to protect thiolase activity). The centrifugation time was increased to 55 min at full speed, in order to insure that free cores (if any) would sediment past the peroxisomes. After centrifugation, the gradients were divided into 18 fractions, which were weighed and analyzed for protein. Samples of the peak of sedimentable protein were fixed for electron microscopy and thiolase was assayed immediately. Other enzyme activities were measured after storage at −20°C. The following experiments were each carried out at least twice.

EXPERIMENT 1: (*a*) Control: peroxisomes were slowly diluted by the dropwise addition of 4 vol of ice-cold distilled water. (*b*) Freezing and thawing: diluted peroxisomes were frozen rapidly in a dry ice/acetone bath and thawed at room temperature. This process was repeated 10 times. (*c*) Sonication: diluted peroxisomes were sonicated 10 times for 30 s in a glass tube in an ice/water bath by means of a Branson Sonifier W-350 (Branson Sonic Power Co., Danbury, CT) equipped with an ultramicro tip (output 2, 50% duty cycle).

EXPERIMENT 2: Pyrophosphate treatment: peroxisomes were diluted with 4 vol of 12.5 mM sodium pyrophosphate, pH 9.0, and stirred gently at 4°C for 18 h as described by Leighton et al. (1). Control: peroxisomes were similarly stirred with distilled water.

EXPERIMENT 3: Triton X-100 treatment: peroxisomes were diluted with Triton X-100 to a final Triton concentration of 0.1%. Control: as in experiment 1, above.

Assays

Catalase (22), cytochrome oxidase (3), esterase (23), urate oxidase (3), acyl-CoA oxidase (24), β-hydroxybutyryl-CoA dehydrogenase (25), thiolase (25), and palmitoyl-CoA synthetase (26) were assayed as described. Units used are in micromoles per minute except that palmitoyl-CoA synthetase is in nanomoles per minute and catalase and cytochrome oxidase, which have first-order reaction kinetics, are expressed in the units defined previously (3). Protein was determined with the Bio-Rad protein assay kit (Bio-Rad Laboratories, Richmond, CA) with bovine serum albumin as standard. The densities of the sucrose gradient fractions were calculated from their refractive indices, which were measured with a Bausch & Lomb refractometer (Bausch & Lomb Inc., Rochester, NY). SDS PAGE was performed as described (27).

Electron Microscopy of Fractions

Samples were fixed with 2% glutaraldehyde (final concentration) in 0.1 M cacodylate buffer (pH 7.4) overnight and pelleted by centrifugation at 45,000 rpm for 30 min in a Beckman 50Ti rotor (Beckman Instruments, Inc., Fullerton, CA). The pellets were postfixed with 1% OsO_4 in 0.1 M cacodylate buffer (pH 7.4) for 1 h, stained with uranyl acetate for 1 h, dehydrated and embedded in Epon 812. Thin sections were stained with uranyl acetate and lead citrate (28) and examined in a Philips 300 electron microscope (Philips Electronic Instruments, Inc., Mahway, NJ) operated at 80 kV (29).

Animals and Materials

Rats were from Charles River Breeding Laboratories (Wilmington, MA). Acyl-CoAs were from Sigma Chemical Co., (St. Louis, MO) and [U-^{14}C]-palmitate was from New England Nuclear (Boston, MA).

RESULTS

Isolation of Peroxisomes in a Vertical Rotor

A light mitochondrial "lambda" fraction, prepared by differential centrifugation (3) (Table I), was subjected to equilibrium-density centrifugation in a sucrose gradient in the vertical TV-856B rotor. As shown in Fig. 1, the peroxisomes (indicated by catalase) were well separated from the mitochondria (cytochrome oxidase). Of the few microsomes present in the lamda fraction (1.8% of those in liver), most were recovered at lower densities than the peroxisomes (Fig. 1). The purity of the peroxisomal fraction was quantitated from the relative specific activities of the marker enzymes (Table I): mitochondria and microsomes each contributed ~3% of the total protein in the peroxisomal fraction, consistent with the purity of ~95% calculated from the catalase relative specific activity.

In agreement with these biochemical data, electron microscopic examination of the peak catalase fraction revealed a nearly homogeneous population of peroxisomes (Fig. 2). Some appear less electron dense than peroxisomes in situ, as if they have lost some of their contents during purification. These results demonstrate that highly purified peroxisomes can be prepared from normal rats in a vertical rotor by a modification of the procedure of Leighton et al. (3). A similar modification has been described by Neat and Osmundsen (30) for the preparation of ~89% pure peroxisomes from the livers of rats in which peroxisome proliferation was induced by clofibrate treatment.

TABLE I. *Peroxisome Isolation in a Vertical Rotor*

Constituent	Marker for	Homogenate activity	Light mitochondrial (lambda) fraction	Peak peroxisome fraction from isopycnic gradient	
					% Purity* [% Contamination]*
		U/g liver	*% of homogenate*	*Relative Sp act*	%
Protein		233 ± 22	4.2 ± 1.5		
Catalase	Peroxisomes	45 ± 5	30 ± 6	36.4 ± 4.4	95 ± 11
Cytochrome oxidase	Mitochondria	24 ± 5	16 ± 10	0.160 ± 0.073	[3.2 ± 1.4]
Esterase	Endoplasmic reticulum	221 ± 74	1.8 ± 0.5	0.161 ± 0.065	[3.2 ± 1.2]

Means ± standard deviations (n = 3).
* Calculated from the relative specific activities as described (6), assuming that mitochondria and endoplasmic reticulum each represent 20% of liver protein.

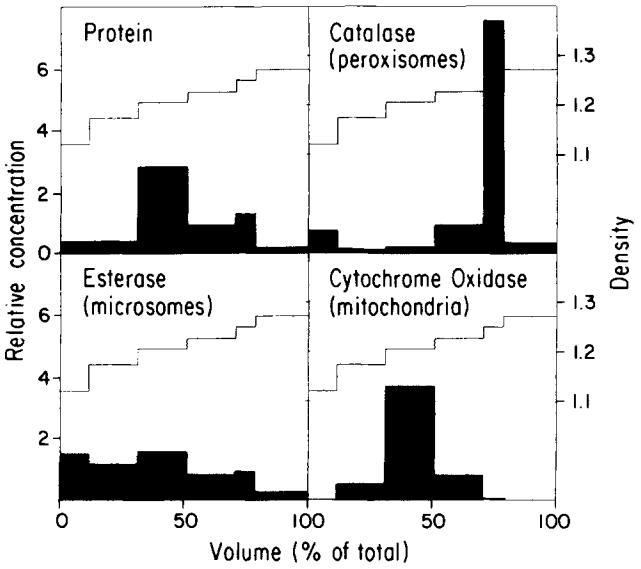

FIGURE 1 Peroxisome preparation in vertical rotor. Isopycnic centrifugation in sucrose of a light mitochondrial (lambda) fraction (see Table I) from normal rat liver. The recoveries varied between 83 and 113%.

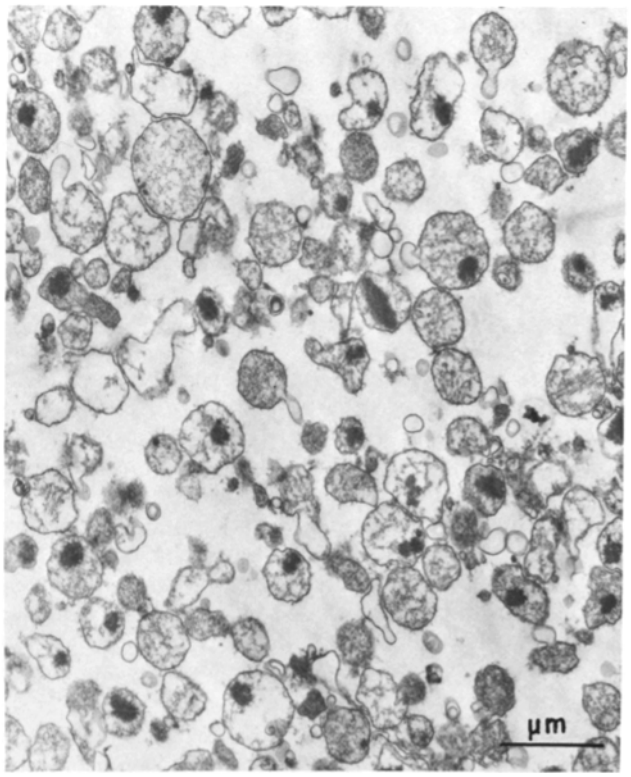

FIGURE 2 Electron micrograph of peroxisomes from the preparative gradient shown in Fig. 1 after a fivefold dilution. Bar, 1 μm; × 14,000.

Recentrifugation of Peroxisomes

Simply diluting the peroxisomes and then recentrifuging them caused the release of some 35% of the protein (Fig. 3*A*). Morphologically, the particles appear more extracted (Fig. 4*a*) than they did as first isolated (Fig. 2), but their membranes are apparently intact and they equilibrate at their usual density of 1.23.

The peroxisomal enzymes were not released in parallel. Thiolase, at one extreme, was 86% soluble, whereas β-hydroxyacyl-CoA dehydrogenase, palmitoyl-CoA synthetase and urate oxidase were entirely retained within the peroxisomes (Fig. 3*A*). Catalase and acyl-CoA oxidase showed intermediate distributions. Soluble catalase (molecular mass ~260 kD [31]) sedimented farther (Fig. 3*A*, fractions 4 and 5) than did soluble thiolase (~78–89 kD [32, 33], fractions 2–4).

SDS PAGE analysis of the gradient fractions revealed similar nonparallel release of peroxisomal polypeptides (Fig. 5*A*). Band *h* was entirely soluble and found mainly in fractions 2 and 3. Bands *d* and *e* were largely soluble, and were concentrated in fractions 4 and 5. Bands *a*, *b*, and *c* were entirely retained within the peroxisomes (Fig. 5*A*, fractions 14 and 15).

The location of the 22-kD peroxisomal integral membrane polypeptide (6) (Fig. 5*A*, 22 kD IMP) could not be ascertained because of anomalously poor resolution in this mass region of this gel (and those of Fig. 9), which caused the 22-kD IMP to co-migrate with a slightly larger soluble protein. Upon reanalysis (Fig. 6*B*), the two proteins were separated normally (6): as expected, the 22-kD IMP was found in the peroxisomes (fraction 15, arrow), and the protein just above it was soluble (fraction 4, arrowhead).

Many of the bands in Fig. 5 have been tentatively identified with peroxisomal enzymes (8, 6, 34) (see also Fig. 6*A*). Band *c* is the bifunctional enoyl-CoA hydratase–β-hydroxyacyl-CoA dehydrogenase (*HD*); the distribution of band *c* by SDS PAGE (Fig. 5*A*) agrees with the distribution of hydratase-

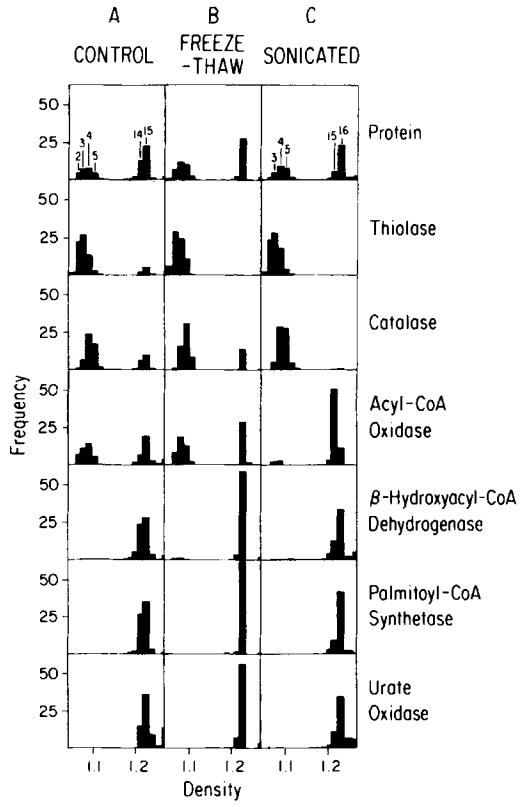

FIGURE 3 Recentrifugation of diluted peroxisome after (*A*) no treatment, (*B*) freezing and thawing 10 times, or (*C*) sonication (ten 30-s bursts). Normalized density distributions according to Leighton et al. (3).

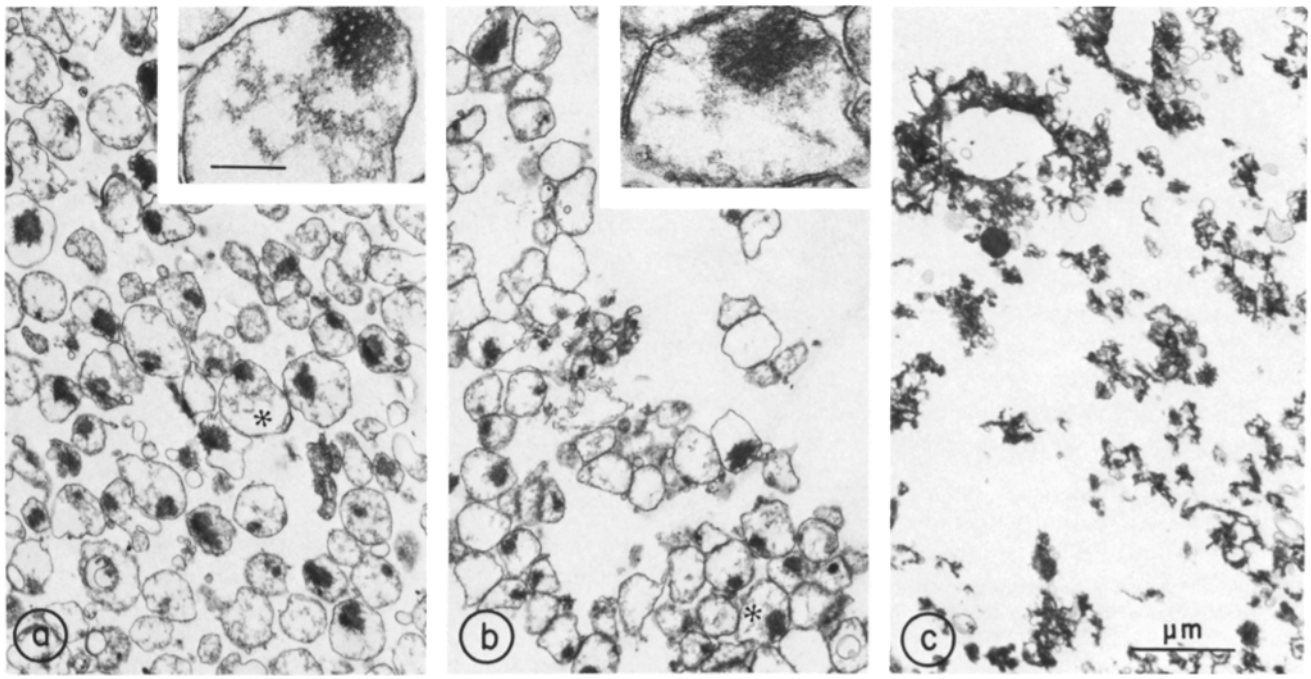

FIGURE 4 Electron micrographs of the dense protein peaks from the experiment of Fig. 3. (*a*) Control, fraction 15; (*b*) frozen and thawed, fraction 15; (c) sonicated, fraction 16. Bar, 1 μm; × 14,000. (Asterisks indicate peroxisomes shown in insets: bar, 200 nm; × 51,000.)

dehydrogenase by enzyme assay (Fig. 3*A*). Similar agreement between SDS PAGE and enzyme assay is observed for catalase (band *e*), urate oxidase (band *g*), acyl-CoA oxidase subunit *b* and probably thiolase (a faint band at ~41 kD [33]). Peroxisome band *d* contains an unrelated protein in addition to acyl-CoA oxidase subunit *a* (35), preventing comparison in this case.

These results demonstrate that the 35% of peroxisomal protein found in soluble form after dilution and recentrifugation of peroxisomes does not result from the rupture of 35% of the peroxisomes with concomitant total loss of their contents. Rather, this is a specific and differential loss of certain enzymes and polypeptides from essentially all the peroxisomes, without discernible membrane damage.

Freezing and Thawing

The purified peroxisomes from the preparative gradient (Figs. 1 and 2) were subjected to 10 cycles of freezing and thawing and then recentrifuged (Fig 3*B*). This treatment increased modestly the release of protein compared to the control (from 35 to 50%). It also increased the soluble percentage of thiolase, catalase, and acyl-CoA oxidase; nonetheless, these three enzymes retained the previously observed hierarchy of solubilization: thiolase > catalase > acyl-CoA oxidase.

Freezing and thawing did not solubilize the dehydrogenase, the synthetase, or the urate oxidase, all of which were found in a sharp peak at a density of 1.226. The treatment substantially inactivated the palmitoyl-CoA synthetase (by 86%, Table II), which was the only serious enzyme inactivation observed in this work. All remaining synthetase activity was found in the dense peak (Fig. 3*B*).

Electron microscopy of this peak (Fig. 4*b*) revealed extensively aggregated peroxisomes that appeared to have less fuzzy fibrillar content than the controls (Fig. 4*a*), but retained cores and apparently intact membranes.

Sonication

Peroxisomes were sonicated vigorously (10 30-s bursts) in order to disrupt their membranes. Remarkably, this did not much affect the distribution of peroxisomal enzymes upon recentrifugation (Fig. 3*C*). Thiolase and catalase were almost completely released from the particles, but acyl-CoA oxidase was much less soluble than without sonication. Acyl-CoA oxidase retained 82% of its activity after sonication (Table II), excluding inactivation of soluble enzyme as the explanation for the shift in the normalized distribution.

SDS PAGE analysis demonstrated that sonication did not greatly change the pattern of soluble and sedimentable polypeptides (Fig. 5*B*). It confirmed the more complete solubilization of catalase (band *e*) and the greater sedimentability of acyl-CoA oxidase subunit *b*. Band *f*, and to a lesser extent, band *h* also shifted from soluble to sedimentable upon sonication.

The surprising morphologic appearance of the sedimentable peak is illustrated in Fig. 4*c*. It consisted of debris and numerous unsealed, apparently everted, membrane fragments covered on one side by abundant amorphous and fibrillar material, sometimes with associated cores. The debris consisted of the same material and cores, in contact. These results demonstrate that the retention of numerous enzymes and polypeptides by peroxisomes after freezing and thawing is not due to their being retained by the membrane. Rather, intermolecular associations attach these proteins to each other and to the membrane, and these bonds persist after the membrane is broken open.

The percentage of soluble protein (38%) was similar to the control (35%), and distinctly less than after freezing and

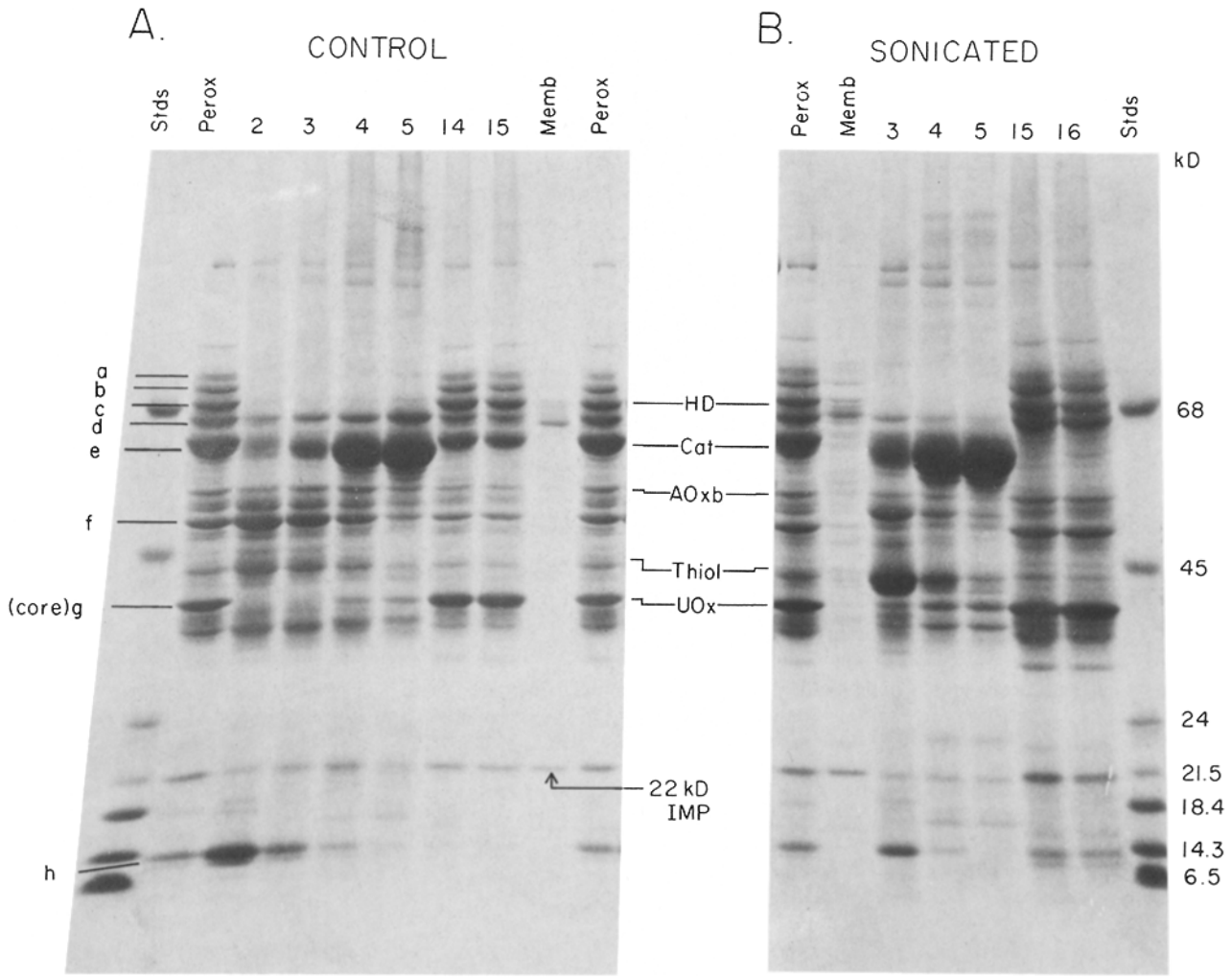

FIGURE 5 SDS PAGE analysis of fractions from recentrifugation of Fig. 3. (*A*) Control. (*B*) Sonicated. Equal amounts of protein (50 μg) from each fraction were analyzed. Fractions identified by numbers as in Fig. 3. Lanes common to this and subsequent gels: (*Perox*) 50 μg normal rat liver peroxisomes (Fig. 1, peak catalase fraction); (Memb) membrane prepared by the carbonate procedure (27) from 80–100 μg of peroxisomal protein; (Stds) molecular mass standards: bovine serum albumin (68 kD), ovalbumin (45 kD), trypsinogen (24 kD), soybean trypsin inhibitor (21.5 kD), β-lactoglobulin (18.4 kD), lysozyme (14.3 kD), and bovine lung trypsin inhibitor (aprotinin) (6.5 kD). Some peroxisomal bands identified at left by letters *a–h*. Positions of peroxisomal enzymes indicated in the center (6, 8): *HD*, bifunctional enoyl-CoA hydratase-β-hydroxyacyl-CoA dehydrogenase; *Cat*, catalase: *AOxb*, acyl-CoA oxidase, subunit b (45); *Thiol*, thiolase; *UOx*, urate oxidase. Anomalous migrations were observed in the 20–23-kD mass region in this gel and in Fig. 9; two peroxisomal proteins migrate together slightly faster than the 21.5-kD standard—normally (6) both migrate more slowly and are resolved—see Fig. 6.

thawing (50%). The density of the sedimentable peak was unaffected by the sonication (Fig. 3). No hint of a lighter membrane fraction was observed, nor were denser, free urate oxidase-containing cores found.

In another experiment with milder sonication, the results closely resembled those of freezing and thawing. Catalase was completely released, acyl-CoA oxidase was 50% soluble, and the synthetase, dehydrogenase, and urate oxidase were quantitatively retained in particles of density 1.23 (not illustrated). Upon observation by electron microscopy, these particles were apparently intact ghosts with fibrillar content. Thus two mechanical treatments (freeze-thaw and mild sonication) have similar effects, and rebinding of acyl-CoA oxidase to the particles only occurs when sonication is vigorous enough to crack the ghosts open.

Pyrophosphate Treatment

Peroxisomes were stirred overnight at 4°C with 10 mM sodium pyrophosphate, pH 9, a procedure shown by Leighton et al. (1) to solubilize most peroxisomal proteins. As a control, peroxisomes were similarly stirred with distilled water.

Stirring alone caused three unexpected results (compare Figs. 7*A* and 3*A*). The median density of the particles decreased from 1.223 to 1.205. β-Hydroxyacyl-CoA dehydrogenase was partially solubilized, accompanied by an increase in soluble protein from 35 to 46%. Some urate oxidase appeared at the bottom of the gradient in fraction 18. Morphologically, stirring alone had no effect except perhaps for some further loss of matrix content (Fig. 8*a* vs. 4*a*). SDS PAGE analysis (Fig. 9*A*) indicated little appreciable change, save for the shift in the bifunctional HD (band *c*) and in another unidentified band at ~29 kD (arrowheads).

Recentrifugation analysis revealed striking changes caused by pyrophosphate (Fig. 7*B*). Four of the six enzymes, including the dehydrogenase, are essentially completely soluble. The sedimentable protein is much less dense, and forms a broad

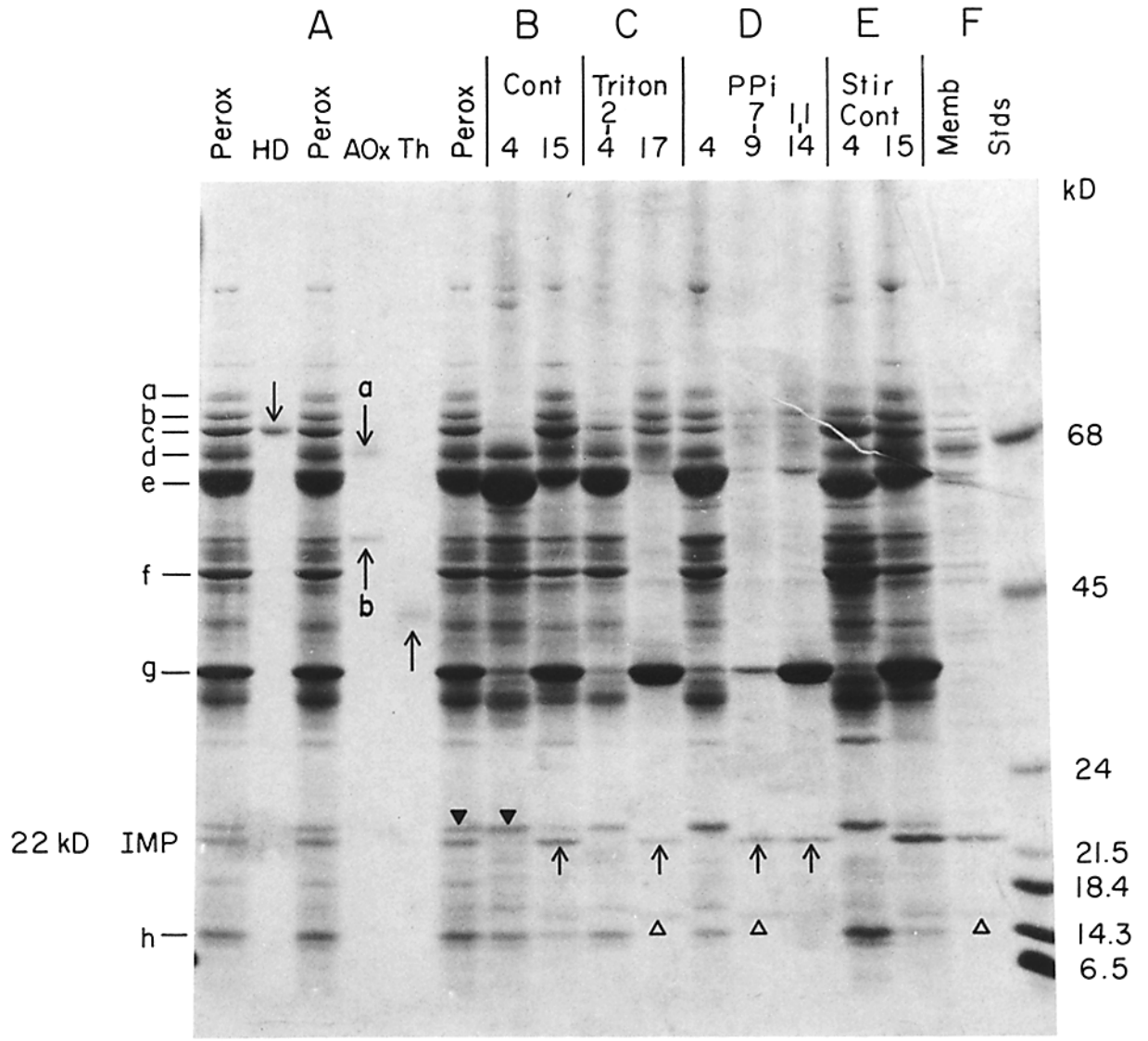

FIGURE 6 SDS PAGE reanalysis with better resolution of the 22-kD region. All lanes contain 50 μg of protein except as indicated. (*A*) Peroxisomes (as in Fig. 5) and purified β-oxidation enzymes (as in reference 8). (*B*) Control: Fig. 3*A*, fractions 4 and 15 (*C*) Triton X-100 experiment: Fig. 10*B*, fractions 2–4 pooled and fraction 17). (*D*) Pyrophosphate experiment: Fig. 7*B*, fractions 4, 7–9 pooled (14 μg) and 11–14 pooled (35 μg). (*E*) Stirring control: Fig. 7*A*, fractions 4 and 15. (*F*) Membrane and standards as in Fig. 5. Arrows in *B–D* indicate the 22-kD integral membrane protein (*IMP*); open arrowheads mark the 15-kD IMP; filled arrowheads indicate a soluble protein that co-migrated with the 22-kD IMP in Figs. 5 and 9. *Th*, thiolase.

peak running through the middle of the gradient. Palmitoyl-CoA synthetase and urate oxidase are both shifted to lighter densities; they form overlapping but noncoincidental peaks in the middle of the gradient.

The SDS PAGE patterns showed equally striking alterations (Fig. 9*B*). Most bands were soluble after the pyrophosphate treatment. Band *g* had a broad distribution through the middle of the gradient, skewed toward the dense side like that of urate oxidase activity. A band that co-migrated with the 22-kD IMP (arrow) was present in the middle of the gradient, but skewed toward the light side. Reanalysis (Fig. 6*D*) verified that this was the integral membrane polypeptide, not the soluble protein with a similar mass. The 15 kD band that was found in several endomembranes (6) was also present in the center of the gradient, apparently skewed to still lighter densities (Fig. 9*B*). Reanalysis of pooled fractions (Fig. 6*D*) clearly showed that the 15 kD IMP was more abundant in the light side of the peak, whereas the core protein (band *g*) was more abundant in the dense side. The 22 kD IMP was in between, as seen before in Fig. 9*B*.

Upon observation by electron microscopy, the particles in the middle of the gradient were sealed peroxisomal membrane ghosts, devoid of content, save for frequent cores and occasional traces of fibrillar material on the inside face of the membrane (Fig. 8*b*). Often the cores were present in a narrow outpouching from the ghosts (insets) suggestive of a tug-of-war between a light vesicle and the dense core during centrifugation.

Triton X-100 Treatment

Triton X-100 caused the disappearance of the peroxisomes at density 1.23; protein and urate oxidase shifted to greater densities (1.264) (Fig. 10*B*). No peroxisomes remained upon observation by electron microscopy; what was observed was cores in association with membrane fragments (Fig. 11). The

TABLE II. *Effect of Treatments on Absolute Activities; Recoveries in Gradients*

	Experiment 1									Experiment 2					
	Control			Frozen/thawed			Sonicated			Stirring control			Pyrophosphate		
	Load	Rec	% Rec	Load	Rec	% Rec	Load	Rec	% Rec	Load	Rec	% Rec	Load	Rec	% Rec
Protein	2.59	2.38	92	1.91	1.68	88	1.86	1.82	98	2.01	1.69	84	2.92	1.95	67
Thiolase	1.44	2.82	196	1.46	1.57	108	1.63	2.13	131	1.12	1.29	115	1.72	1.18	69
Catalase	27.0	20.3	75	25.4	20.2	80	24.6	21.2	86	20.6	19.3	94	34.5	24.3	70
Acyl-CoA oxidase	0.49	0.40	82	0.25	0.33	131	0.40	0.31	78	0.29	0.30	103	0.41	0.46	112
β-Hydroxyacyl-CoA dehydrogenase	1.78	2.17	122	1.78	1.95	110	1.41	0.74	53	2.82	2.78	98	3.24	2.27	70
Palmitoyl-CoA synthetase	22.4	30.3	135	3.17	4.88	154	22.4	12.1	54	29.9	29.4	98	31.4	26.4	84
Urate oxidase	1.64	1.44	88	0.76	1.08	142	1.12	1.17	104	1.52	0.96	63	1.70	1.20	71

Rec, recovery.

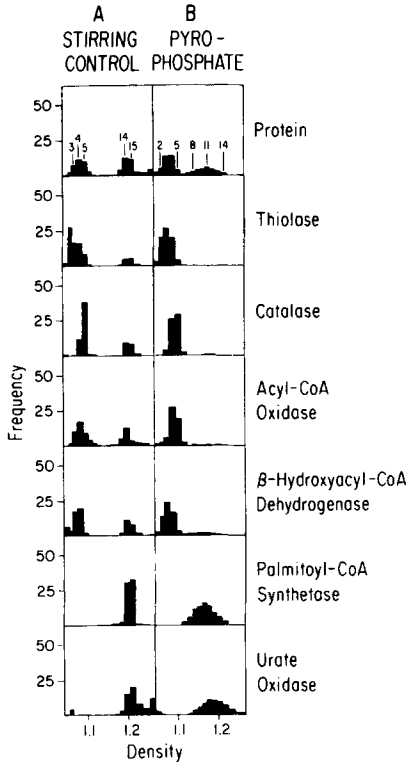

FIGURE 7 (*A*) Control peroxisomes were stirred as in *B* but with distilled water. (*B*) Recentrifugation of peroxisomes after pyrophosphate treatment. Peroxisomes were stirred in 10 mM sodium pyrophosphate, pH 9, for 18 h at 4°C.

dense fraction and the soluble material were compared by SDS PAGE under conditions of optimal resolution in the 22-kD region (Fig. 6*C*). The 22-kD integral membrane polypeptide (arrow) was found entirely in the dense fraction 17 with band *g* (the core protein) in agreement with the electron microscopic results. Several other proteins were likewise not solubilized by Triton X-100, including bands *a* and *b* and the 15-kD IMP (arrowhead). These results demonstrate that Triton X-100 fragments, but does not solubilize, the peroxisomal membrane.

A 10-fold lower concentration of Triton X-100 (0.01%) released ~34% of the urate oxidase which sedimented to the bottom of the gradient (not shown). The cores were not accompanied by β-hydroxyacyl-CoA dehydrogenase activity, which was found entirely in peroxisomes (density 1.225).

DISCUSSION

Intraperoxisomal Locations of the Enzymes

The release of the enzymes by the various treatments is summarized in Fig. 12.

MATRIX: Thiolase and catalase largely leak out of peroxisomes even in the controls; the treatments increase their release to nearly 100%. We infer that they are soluble within the peroxisomal matrix (Table III). Acyl-CoA oxidase tends to follow catalase: both are ~65% soluble in the control and ~90% released after pyrophosphate treatment. However, the mechanical treatments that promote catalase leakage cause acyl-CoA oxidase retention (or readsorption). This is not due to binding to the cores because in the stirring control (Fig. 7A) acyl-CoA oxidase is not associated with urate oxidase in the bottom fraction. Sonication causes the oxidase to become reassociated with the damaged peroxisomes, perhaps adsorbing on the exposed amorphous material seen in Fig. 4*c*. No loss of activity is associated with this change in location. One possibility is that the acyl-CoA oxidase is amphipathic and has two states (both active) with different affinities for the other peroxisomal proteins. Alternatively, there might be two acyl-CoA oxidases, one of which never leaks out of peroxisomes except when pyrophosphate-treated, and the other which always leaks out but can be readsorbed upon sonication. In any case, we assign acyl-CoA oxidase to the peroxisome matrix, but note its variable association with the insoluble structure. Some Coomassie Blue-stained polypeptides (bands *d*, *f*, and *h*) likewise qualify as matrix proteins on the basis of their distributions after the several treatments.

MATRIX—POORLY SOLUBLE: β-Hydroxyacyl-CoA dehydrogenase remains tightly bound to the particles in the control, freeze-thawing, and sonication experiments (Fig. 12), but it is neither a core protein nor firmly anchored in the membrane because it is released from both these structures by stirring, pyrophosphate, and Triton X-100. It appears to be a poorly soluble matrix protein. Its lack of solubility may be due to aggregation with itself (or other matrix proteins) to form large oligomers, or to binding to the core or to the membrane, or more than one of the above. By electron microscopic immunocytochemistry, it is found throughout the peroxisomal matrix (15, 16). It appears likely that the dehydrogenase is in the fibrillar or amorphous material observed morphologically in Fig. 4, *a–c*, which seems to be attached to both cores and membrane. Indeed, in the sonication-broken peroxisomes (Fig. 4*c*), this material may be the only thing connecting cores and membranes; were the cores

TABLE II (continued)

Experiment 3					
Control			Triton X-100		
Load	Rec	% Rec	Load	Rec	% Rec
1.64	1.68	102	2.1	2.0	95
11.0	11.1	101	15.2	14.8	97
1.71	1.36	80	1.57	0.94	60
0.80	0.56	70	0.82	0.64	78

completely free, they would be expected to sediment to the bottom of the gradient. Whether this material was fibrillar in vivo or its appearance is an artefact of preparation for microscopy is unknown.

Other polypeptides, notably bands *a* and *b* and the 29-kD band follow the dehydrogenase (band *c*) in most of these experiments. These are likewise not integral membrane proteins (6).

Of the 50% of the protein retained in peroxisomes after freezing and thawing, the core constitutes 10% (1) and the integral membrane proteins 12% (6). The balance (28%) is presumably the "poorly soluble matrix proteins" and peripheral membrane proteins. Of this, a third to a half (9–15% of total peroxisomal protein) was solubilized by pyrophosphate or Triton X-100.

MEMBRANE AND CORE: Urate oxidase (the major, if not only, core protein) (1, 7, 17–19) and palmitoyl-CoA synthetase (reportedly a membrane protein) (36) were not released in soluble form in any of these experiments (Fig. 12). Cores and membranes (or membrane fragments) were found together in all the fractions examined by electron microscopy (even those treated with Triton X-100). Urate oxidase and palmitoyl-CoA synthetase were partially separated after pyrophosphate treatment: the two activities exhibited broad overlapping peaks (Fig. 7*B*). The location of the membrane in this experiment may be inferred from the position of the 22-kD integral peroxisomal membrane polypeptide, which is concentrated in fractions 8–11, with a maximum in fractions 10 and 11 (arrows) (Fig. 9*B*). The distribution of the 22-kD IMP was quantitated by scanning the gel (Fig. 13, *A* and *B*). It resembles that of palmitoyl-CoA synthetase (median densities 1.167 and 1.166). The similarly was confirmed by linear combination analysis according to Krisans et al. (26) (Fig. 13*C*). This demonstrates that the synthetase is a membrane protein, in agreement with the conclusion of Mannaerts et al. (36), which was inferred from different evidence.

As expected, the band *g* (core protein) distribution closely resembles the urate oxidase activity distribution (1.184 vs. 1.187 median densities). We suspect that the increase in core protein relative to membrane protein with increasing equilibrium density reflects the fractionation of peroxisomal ghosts according to the size of their core.

Biogenesis

The existence of a sizable class of poorly soluble peroxisomal matrix proteins lends some support to the suggestion that self-assembly could contribute to peroxisome biogenesis (37). If the newly made proteins can permeate through the peroxisomal membrane, retention within by oligomerization would be sufficient to explain posttranslational import.

After a variety of treatments that released from 35 to 55%

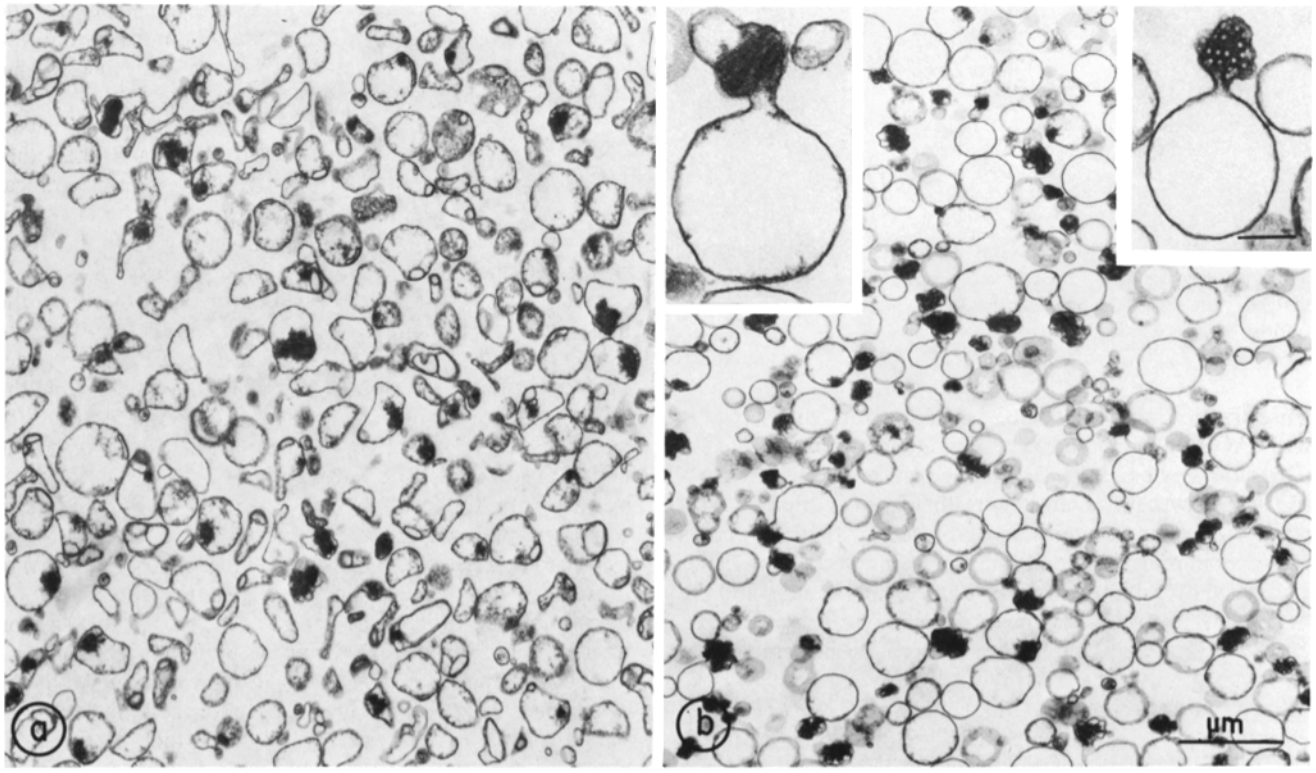

FIGURE 8 Electron microscopy of dense protein peaks from the experiment of Fig. 7 (a) Control stirring, pooled fractions 14 and 15. (*b*) Pyrophosphate-treated, pooled fractions 9–12. Bar, 1 μm; × 14,000. ([*Inset*] Bar, 200 nm; × 43,000.)

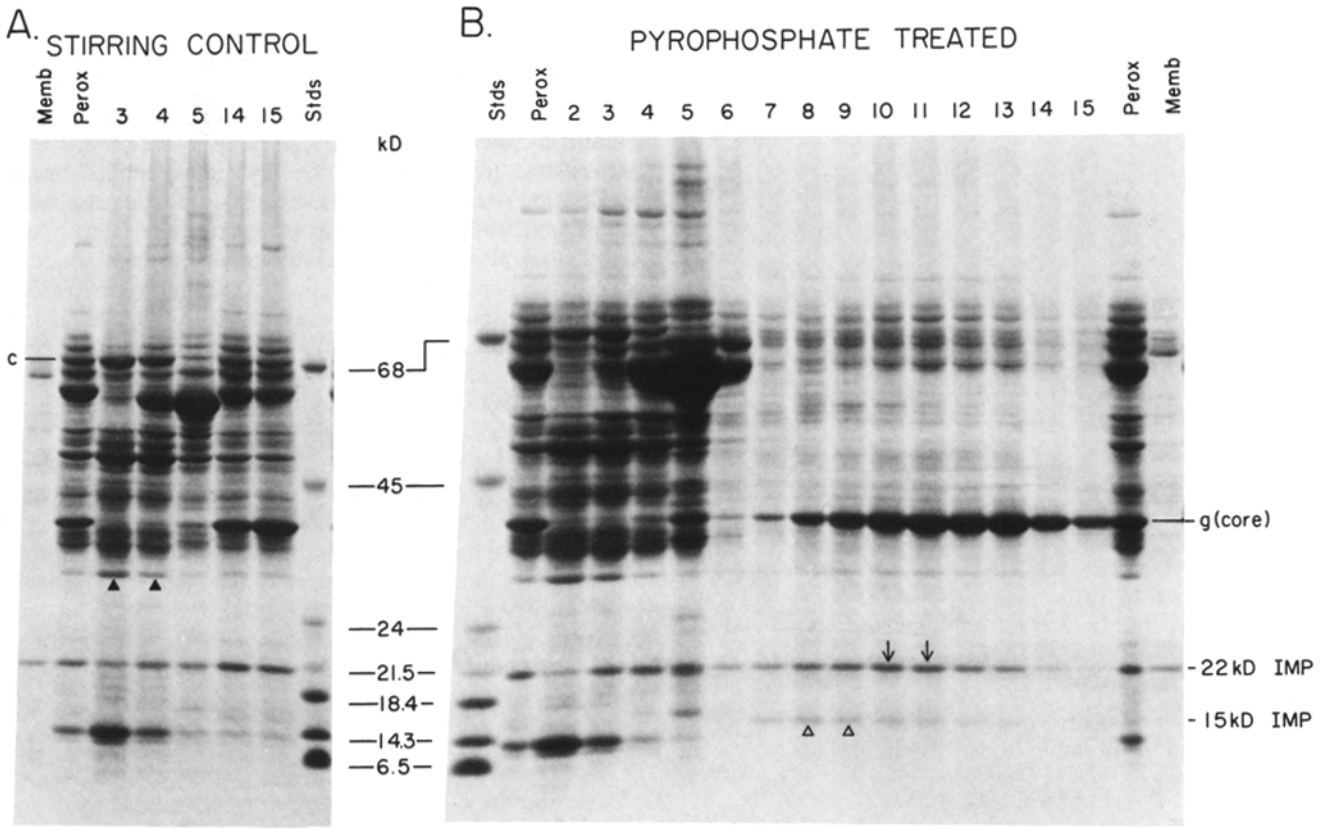

FIGURE 9 SDS PAGE analyses of (*B*) pyrophosphate treatment and (*A*) stirring control. Fraction numbers as in Fig. 7. A 350-μl sample of each fraction was analyzed after trichloroacetic acid precipitation, except for fractions 3 and 4 from which only 100 or 120 μl (50 μg of protein) was taken.

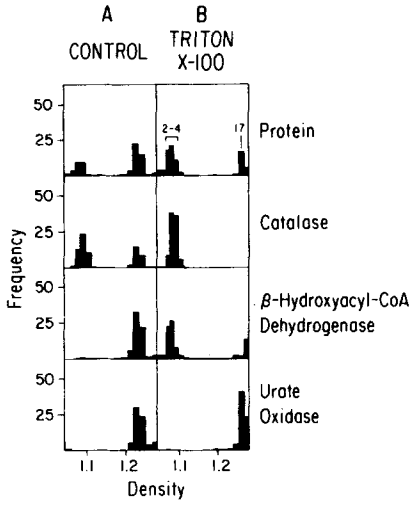

FIGURE 10 (*A*) Control peroxisomes were diluted with water. (*B*) Recentrifugation of peroxisomes after 0.1% Triton X-100 treatment.

of the total proteins, the membranes still appeared to be intact. Probably the membranes rupture and then reseal. Less likely, but worth considering, is the egress of soluble proteins through intact membranes. After a change in internal milieu after isolation in sucrose gradients (or pyrophosphate treatment), peroxisomal proteins could disaggregate and leave the way they came. Newly made proteins are known to enter peroxisomes posttranslationally through apparently intact membranes (5, 20, 35, 38, 39). The presumed unidirectionality of transport is not experimentally documented.

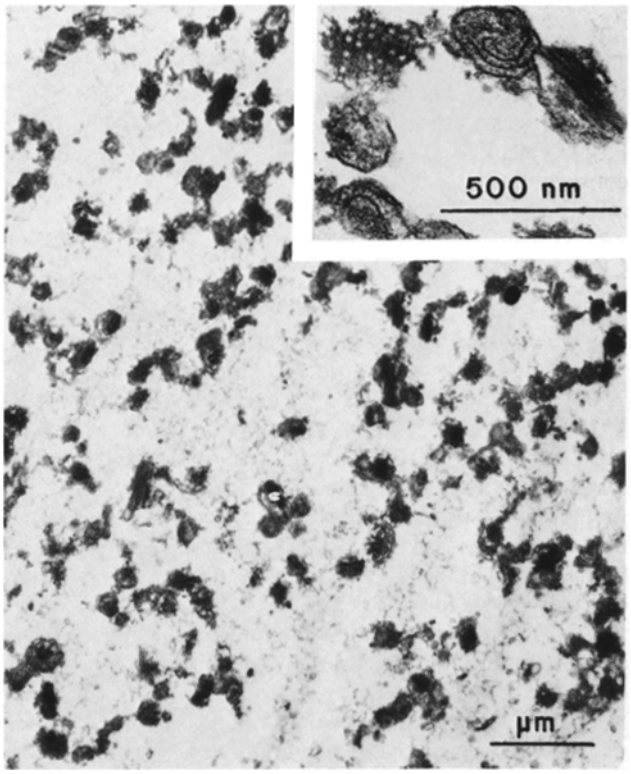

FIGURE 11 Electron microscopy of dense protein peak from the experiment of Fig. 10, fraction 17. Bar, 1 μm; × 14,000. ([*Inset*] Bar, 500 nm; × 48,000.)

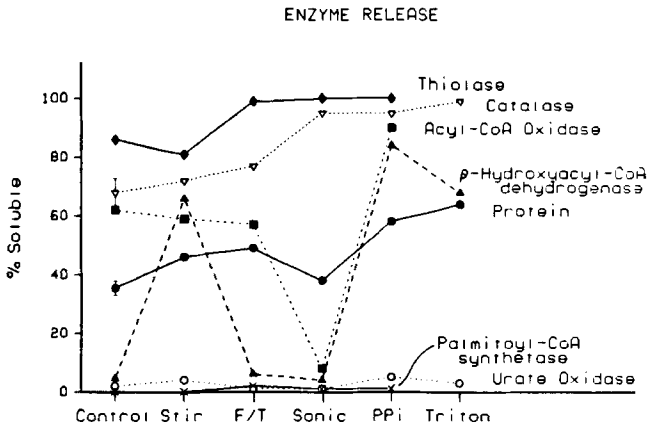

FIGURE 12 Summary of solubilization of enzymes by various treatments. The soluble activity (leftmost six fractions in Figs. 3, 7, and 10) is expressed as a fraction of the total recovered activity.

TABLE III. *Intraperoxisomal Localization of Enzymes and Polypeptides*

Intraorganellar site	Enzyme or polypeptide band
Matrix	
Soluble	Thiolase, catalase, band *h*
Intermediate	Acyl-CoA oxidase, bands *d, f*
Poorly soluble	Hydratase-dehydrogenase, bands *a, b*, 29 kD
Membrane	Palmitoyl-CoA synthetase, 22- and 15-kD integral membrane polypeptides
Core	Urate oxidase

Analytical Cell Fractionations

Catalase is a convenient marker enzyme for peroxisomes. The observation that it escapes readily from peroxisomes supports previous conclusions that, at least in rat liver, soluble catalase escaped from peroxisomes at homogenization (3, 5). Future calculations of peroxisomal activities must take into consideration the differential leakiness of peroxisomal enzymes.

Comparison with Other Reports

A number of investigators have studied the intraperoxisomal location of enzymes by a variety of techniques. All workers agree that urate oxidase is located in the core (1, 3, 7, 17–19) and that catalase is soluble in the matrix (1, 11, 13, 40). Our finding that thiolase is also soluble is consistent with similar findings by Hayashi et al. (14) with LK-903-treated rats and Huttinger et al. (13) with clofibrate-treated rats. Other members of the class of soluble matrix proteins include L-α-hydroxyacid oxidase (1, 5, 11, 40), carnitine acetyltransferase (41), and carnitine octanoyltransferase (41). D-amino acid oxidase appears to follow catalase closely in some (3, 42) but not all (22) cell fractionation experiments and upon freezing and thawing (1), but was not fully solubilized in other disruption experiments (11, 14).

The intraperoxisomal localization of β-hydroxyacyl-CoA dehydrogenase has been more controversial, probably because of its unusual behavior. The conclusions that it is soluble (13) or firmly bound to the core (14) appear to reflect the different approaches that were used. The data themselves are in reasonable agreement with those reported here, and are consistent with the conclusion that the dehydrogenase is a poorly soluble matrix protein.

Acyl-CoA oxidase has been reported to be soluble (13) or to be weakly associated with the core (14). The entire β-oxidation system has also been reported to be soluble (12), (which probably reflects the rate-limiting oxidase). A matrix localization is supported by the results of Inestrosa et al. (43), who found similar proportions of soluble and sedimentable acyl-CoA oxidase and catalase when a liver homogenate from a nafenopin-treated rat was centrifuged into a metrizamide gradient. The present results also imply a matrix localization; although a portion of the enzyme is poorly soluble, it does not bind to cores.

The retention by castor bean glyoxysome ghosts of 60% of the β-hydroxyacyl-CoA dehydrogenase but only 10% of the thiolase (44) is similar to what we observe with rat liver peroxisomes. Also similar is the solubilization of the glyoxysomal dehydrogenase by a modest increase in ionic strength (44). Although these data were interpreted in terms of a loose membrane association, they are not inconsistent with a local-

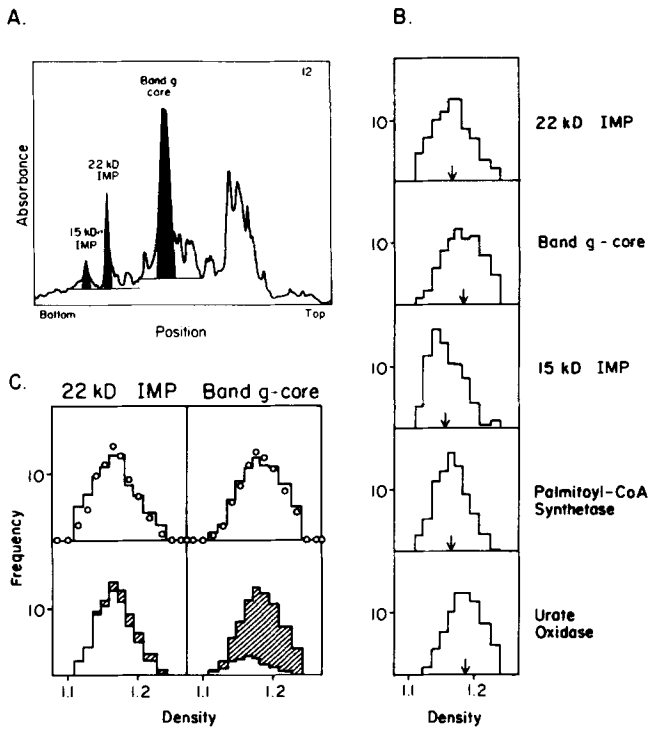

FIGURE 13 Comparison of distributions of polypeptides and enzymes after pyrophosphate treatment. (*A*) A photograph of the SDS PAGE data of Fig. 9 was scanned with a Bio-Rad model 1650 densitometer and the peaks were integrated by triangulation. The scan of fraction 12 is illustrated. (*B*) Distributions of the polypeptides in fractions 6–15 determined by scanning and the distributions of palmitoyl-CoA synthetase and urate oxidase activity in the same region of the gradient (from Fig. 7*B*). (*C*) Calculation of the polypeptide distributions as linear combinations of the enzyme distributions. *Left*: 22-kD integral membrane polypeptide. *Right*: core protein (band *g*). *Lower panels*: linear combinations of palmitoyl-CoA synthetase activity (*no shading*) and of urate oxidase activity (*hatched*). *Upper panels*: the sums of the calculated optimal linear combinations are represented as circles on the measured polypeptide band distributions. The calculated coefficients were: 22-kD IMP—79% synthetase + 12% urate oxidase; core protein—18% synthetase + 78% urate oxidase. See Krisans et al. (26) for further details about the linear combinations.

ization in the fibrillar material that is seen in the glyoxysome ghosts just as we see it in peroxisome ghosts.

We thank Stanley Fowler (University of South Carolina) for information from an unpublished experiment on the preparation of peroxisomes in a vertical rotor.

This research was supported by National Science Foundation grant PCM82-08315 and by National Institutes of Health grant AM 19394. Stefan Alexson was supported by a grant to Dr. Barbara Cannon from the Swedish National Science Research Council and a travel grant from Knut and Alice Wallenberg's Jubileumsfond. Paul B. Lazarow was the recipient of an Established Fellowship from the New York Heart Association.

Received for publication 19 September 1984, and in revised form 31 January 1985.

REFERENCES

1. Leighton, F., B. Poole, P. B. Lazarow, and C. de Duve. 1969. The synthesis and turnover of rat liver peroxisomes. I. Fractionation of peroxisome proteins. *J. Cell Biol.* 41:521–535.
2. Beaufay, H., P. Jacques, P. Baudhuin, O. Z. Sellinger, J. Berthet, and C. de Duve. 1964. Tissue fractionation studies. 18. Resolution of mitochondrial fractions from rat liver into three distinct populations of cytoplasmic particles by means of density equilibration in various gradients. *Biochem. J.* 92:184–205.
3. Leighton, F., B. Poole, H. Beaufay, P. Baudhuin, J. W. Coffey, S. Fowler, and C. De Duve. 1968. The large scale separation of peroxisomes, mitochondria and lysosomes from the livers of rats injected with Triton WR-1339. *J. Cell Biol.* 37:482–513.
4. Poole, B., T. Higashi, and C. de Duve. 1970. The synthesis and turnover of rat liver peroxisomes. III. The size distribution of peroxisomes and the incorporation of new catalase. *J. Cell Biol.* 45:408–415.
5. Lazarow, P. B., and C. de Duve. 1973. The synthesis and turnover of rat liver peroxisomes. V. Intracellular pathway of catalase synthesis. *J. Cell Biol.* 59:507–524.
6. Fujiki, Y., S. Fowler, H. Shio, A. L. Hubbard, and P. B. Lazarow. 1982. Polypeptide and phospholipid composition of the membrane of rat liver peroxisomes. Comparison with endoplasmic reticulum and mitochodrial membranes. *J. Cell Biol.* 93:103–110.
7. Antonenkov, V. D., and and L. F. Panchenko. 1978. Organization of urate oxidase in peroxisomal nucleoids. *FEBS (Fed. Eur. Biochem. Soc.) Lett.* 88:151–154.
8. Lazarow, P. B., Y. Fujiki, R. Mortensen, and T. Hashimoto. 1982. Identification of β-oxidation enzymes among peroxisomal polypeptides: increase in Coomassie Blue-stainable protein after clofibrate treatment. *FEBS (Fed. Eur. Biochem. Soc.) Lett.* 150:307–310.
9. Mortensen, R. M. 1983. Clofibrate-induced increases in peroxisomal proteins: Effects on synthesis, degradation, and mRNA activity. Thesis. The Rockefeller University, New York.
10. Osumi, T., and T. Hashimoto. 1979. Peroxisomal β-oxidation system of rat liver. Copurification of enoyl-CoA hydratase and 3-hydroxyacyl-CoA dehydrogenase. *Biochem. Biophys. Res. Commun.* 89:580–584.
11. Hayashi, H., T. Suga, and S. Niinobe. 1971. Studies on peroxisomes. I. Intraparticulate localization of peroxisomal enzymes in rat liver. *Biochim. Biophys. Acta.* 252:58–68.
12. Appelkvist, E. L., and G. Dallner. 1980. Possible involvement of fatty acid binding protein in peroxisomal β-oxidation of fatty acids. *Biochim. Biophys. Acta.* 617:156–160.
13. Huttinger, M., H. Goldenberg, and R. Kramar. 1980. Intraparticulate localization of the peroxisomal fatty acid β-oxidation system in rat liver. *Hoppe-Seyler's Z. Physiol. Chem.* 361:1125–1128.
14. Hayashi, H., S. Hino, and F. Yamasaki. 1981. Intraparticulate localization of some peroxisomal enzymes related to fatty acid β-oxidation. *Eur. J. Biochem.* 120:47–51.
15. Reddy, J. K., M. Bendayan, and M. K. Reddy. 1982. Immunocytochemical localization of catalase, heat-labile enoyl-CoA hydratase, and polypeptide PPA-80 in rat liver. *Ann. NY. Acad. Sci.* 386:495–498.
16. Yokota, S., T. Hashimoto, and H. D. Fahimi. 1983. Fatty acid beta-oxidation enzymes in peroxisomes: comparison of localization by pre- and postembedding immunocytochemical techniques. *Fed. Proc.* 42:1303.
17. Hruban, Z., and H. Swift. 1964. Uricase: localization in hepatic microbodies. *Science (Wash. DC.)* 146:1316–1318.
18. Tsukada, H., Y. Mochizuki, and S. Fujiwara. 1966. The nucleoids of rat liver cell microbodies. Fine structure and enzymes. *J. Cell Biol.* 28:449–460.
19. Hayashi, H., K. Taya, T. Suga, and S. Niinobe. 1976. Studies on peroxisomes. VI. Relationship between the peroxisomal core and urate oxidase. *J. Biochem.* 79:1029–1034.
20. Lazarow, P. B., and M. Robbi, Y. Fujiki, and L. Wong. 1982. Biogenesis of peroxisomal proteins in vivo and in vitro. *Ann. NY. Acad. Sci.* 386:285–300.
21. Alexson, S., H. Shio, and P. B. Lazarow. 1982. Intraperoxisomal localication of β-oxidation enzymes in rat liver. *Hoppe-Seyler's Z. Physiol. Chem.* 363:968–969.
22. Baudhuin, P., H. Beaufay, Y. Rahman-Li, O. Z. Sellinger, R. Wattiaux, P. Jacques, and C. de Duve. 1964. Tissue fractionation studies. 17. Intracellular distribution of monomaine oxidase, aspartate aminotransferase, alanine aminotransferase, D-amino acid oxidase and catalase in rat-liver tissue. *Biochem. J.* 92:179–184.
23. Beaufay, H., A. Amar-Costesec, E. Feytmans, D. Thines-Sempoux, M. Wibo, M. Robbi, and J. Berthet. 1974. Analytical study of microsomes and isolated subcellular membranes from rat liver. I. Biochemical methods. *J. Cell Biol.* 61:188–200.
24. Lazarow, P. B., and C. de Duve. 1976. A fatty acyl-CoA oxidizing system in rat liver peroxisomes; enhancement by clofibrate, a hypolipidemic drug. *Proc. Natl. Acad. Sci. USA.* 73:2043–2046.
25. Lazarow, P. B. 1978. Rat liver peroxisomes catalyze the β-oxidation of fatty acids. *J. Biol. Chem.* 253:1522–1528.
26. Krisans, S., R. M. Mortensen, and P. B. Lazarow. 1980. Acyl-CoA synthetase in rat liver peroxisomes. Computer-assisted analysis of cell fractionation experiments. *J. Biol. Chem.* 255:9599–9607.
27. Fujiki, Y., A. L. Hubbard, S. Fowler, and P. B. Lazarow. 1982. Isolation of intracellular membranes by means of sodium carbonate treatment. Application to endoplasmic reticulum. *J. Cell Biol.* 93:97–102.
28. Reynolds, E. S. 1963. The use of lead citrate at high pH as an electron-opaque stain in electron microscopy. *J. Cell Biol.* 17:208–213.
29. Shio, H., and P. B. Lazarow. 1981. Relationship between peroxisomes and endoplasmic reticulum investigated by combined catalase and glucose-6-phosphatase cytochemistry. *J. Histochem. Cytochem.* 29:1263–1272.
30. Neat, C. E., and H. Osmundsen. 1979. The rapid preparation of peroxisomes from rat liver by using a vertical rotor. *Biochem. J.* 180:445–448.
31. Robbi, M., and P. B. Lazarow. 1978. Synthesis of catalase in two cell-free protein-synthesizing systems and in rat liver. *Proc. Natl. Acad. Sci. USA.* 75:4344–4348.
32. Miyazawa, S., S. Furuta, T. Osumi, T. Hashimoto, and N. Ui. 1981. Properties of peroxisomal 3-ketoacyl-CoA thiolase from rat liver. *J. Biochem.* 90:511–519.
33. Fujiki, Y., R. A. Rachubinski, R. M. Mortensen, and P. B. Lazarow. 1985. Synthesis of 3-ketoacyl-CoA thiolase of rat liver peroxisomes on free polyribosomes as a larger precursor. Induction of thiolase mRNA activity by clofibrate. *Biochem. J.* 226:697–704.
34. Robbi, M., and P. B. Lazarow. 1982. Peptide mapping of peroxisomal catalase and its precursor: comparison to the primary wheat germ translation product. *J. Biol. Chem.* 257:964–970.
35. Fujiki, Y., and P. B. Lazarow. 1985. Post-translational import of fatty acyl-CoA oxidase and catalase into peroxisomes of rat liver *in vitro*. *J. Biol. Chem.* 260:5603–5609.
36. Mannaerts, G. P., P. Van Veldhoven, A. Van Broekhoven, G. Vandebroek, and L. J. Debeer. 1982. Evidence that peroxisomal acyl-CoA synthetase is located at the cytoplasmic side of the peroxisomal membrane. *Biochem. J.* 204:17–23.
37. Lazarow, P. B. 1980. Properties of the natural precursor of catalase: implications for peroxisome biogenesis. *Ann. NY. Acad. Sci.* 343:293–303.
38. Lazarow, P. B., H. Shio, and M. Robbi. 1980. Biogenesis of peroxisomes and the peroxisome reticulum hypothesis. *In* 31st Mosbach Colloquium. Biological Chemistry of Organelle Formation. T. Bucher, W. Sebald, and H. Weiss. editors. Springer-Verlag, New York. 187–206.
39. Miura, S., M. Mori, M. Takiguchi, M. Tatibana, S. Furuta, S. Miyazawa, and T. Hashimoto. 1984. Biosynthesis and intracellular transport of enzymes of peroxisomal β-oxidation. *J. Biol. Chem.* 259:6397–6402.
40. Antonenkov, V. D., and A. M. Gerassimov. 1978. Enzymological study of the structural organization of the peroxisomal matrix in rat liver. *Tsitologiya* 20:676–681.
41. Markwell, M. A. K., N. E. Tolbert, and L. L. Beiber. 1976. Comparison of the carnitine acyltransferase activities from rat liver peroxisomes and microsomes. *Arch. Biochem. Biophys.* 176:479–488.
42. de Duve, C., and P. Baudhuin. 1966. Peroxisomes (microbodies and related particles). *Physiol. Rev.* 46:323–357.
43. Inestrosa, N. C., M. Bronfman, and F. Leighton. 1979. Properties of fatty acyl-CoA oxidase from rat liver, a peroxisomal flavoprotein. *Life Sci.* 25:1127–1136.
44. Huang, A. H. C., and H. Beevers. 1973. Localization of enzymes within microbodies. *J. Cell Biol.* 58:379–389.
45. Osumi, T., T. Hashimoto, and N. Ui. 1980. Purification and properties of acyl-CoA oxidase from rat liver. *J. Biochem.* 87:1735–1746.